Journal of the Serbian Society for Computational Mechanics / Vol. 2 / No. 1, 2008 / pp. 44-62

UDC: 531:519.673

On a Reliable Finite Element Approach in Multiscale Multimaterial Solid Thermo-Mechanics

D. Mijuca

Faculty of Civil Construction Management, University UNION,
Cara Dusana 62--64, 11000 Belgrade, Serbia
dmijuca@matf.bg.ac.yu

Abstract

This paper presents an original time efficient primal-mixed finite element approach in the geometrically *multiscale* solid thermo-mechanics. It will be shown that present finite element HC8/27 passes second stability condition (inf-sup test) for highly distorted finite elements with aspect ratio up to 7 orders of magnitude, for both, compressible and nearly incompressible materials. The semi-coupling between thermal and mechanical physical fields is achieved straightforwardly via essential boundary condition per stress, and without *consistency* error. The direct sparse solver and matrix scaling routine are used for the solution of resulting large scale indefinite systems of linear equations. A number of pathological benchmark model problems, with material interfaces or coating, with geometrical scale resolutions up to 8 orders of magnitude and aspect ratio of finite elements up to 7 orders of magnitude, are examined to test the reliability. A new definition of multiscale reliability is given. It will be shown how dimensional reduction theories can drastically deteriorate the place and intensity of maximal stress results, which can lead to a premature structure failure. In addition, bridging of continuum (finite element) and atomistic (molecular dynamics) mechanics is more accurate if continuum approach is based on a reliable fully three-dimensional numerical approach, mainly because it prevails spurious results and enables extension of the continuum region deep toward the atomistic scale.

Keywords: solid mechanics, dimensional reduction, finite element, multiscale, geometric invariance, incompressible limit, residual stresses1.

1. Introduction

It is widely recognized that there is a need for a straightforward, consistent, reliable and time-efficient numerical simulation procedure for multiscale multimaterial model problems in order to provide accurate data about the state of stress and defect structure of materials under thermo-mechanical loading.

Although the standard, *primal* finite-element (FE) method has been heavily used by the engineering community for more than five decades, it does not have its full application in a geometrically multiscale analysis. This is primarily due to numerous problems regarding stability (see Bathe 1996, Arnold 1990, Robey 1992) of finite elements when they are extremely

distorted, thin or become incompressible. For example, when a primal finite element approach is based on the dimensional reduction, see Babuska (1981), it can suffer from hourglass locking (see Bathe 1996, Chavan et al. 2007). In addition, for nearly incompressible materials there are spurious oscillations of stresses due to the volumetric locking. These problems may be divided in three main groups. The first group of problems is related to shear locking when low order elements are used. The second group of problems displays the presence of spurious or kinematic modes, i.e. extra zeroes eigenvalues of system matrix, when a selectively reduced integration is used. The third group of problems represents the occurring of nearly singular system matrix when the limit of incompressibility is approached. The popular *standard displacement-based finite element approach*, as the representative of the class of primal approaches, in its *raw* form is not applicable in these situations. In spite of a large number of techniques to remedy these bad characteristics, they are all on the account of violation of the consistency and stability issues. For example, a very popular general shell element QUAD is not stable in the analysis of banding dominated problems, see Piltner (2001), regardless of number of local nodes per element.

When it comes to numerical simulation, i.e. approximation of the mathematical model given by differential equations by a chosen numerical method, the accuracy of the numerical results strongly depends on the reliability of the numerical scheme, quality of the material's characterization and model idealization (dimensional reduction and detail suppression technique). The finite element (FE) method is certainly the first numerical method of choice in the thermo-mechanical analysis of solid bodies for several decades. Although, theoretical settings of different approaches, as primal, mixed and hybrid, were simultaneously developed, only the primal approach, were there is only one solution variable, gained notable attention of the industry and commercial software developers. In addition, the finite elements based on the dimensional reduction theories (beam and plane) are still the most used elements. It is primarily due to the limitation of the speed of the available computer recourses and the opinion that is not possible to develop reliable mixed approaches in which displacement and stresses are simultaneous calculated.

Nevertheless, new materials, as composite sandwiched plates with foam in its core, functionally graded materials, and analysis at higher temperatures (fire) when material properties drastically change, require the fully 3D reliable numerical procedure toward incompressibility, see Djoko (2006). Next, the use of mixed/hybrid FE approaches, see Rannacher (1997) and Arnol (1990), is favorable because of the possibility to introduce a priori known stresses, as residual, directly in calculation as the known initial conditions. It is opposite to primal approaches (e.g. displacement finite element method) in which initial stresses are introduced as a contribution to the force vector, while the residual stresses are simply added a posteriori to calculated stresses, which entails a lost accuracy and is applicable only in the elastic range.

Further, when the state of initial stress is heterogeneous along the thickness, it is not possible to use plate theories, even if the implemented theory is mixed. The next reason against the use of plane theories are the so-called locking effects which slow the convergence, see Maksimyuk1 (2004). A similar effect, called volumetric or dilatational locking, is widely known in relation to weakly compressible bodies. Under certain conditions, even the classical model based on the Kirchoff–Love hypotheses may lead to the membrane locking. Although there are new approaches proposed to improve the convergence of numerical solution for new classes of problems as thin and non-thin shells with a curvilinear (circular, elliptical) hole, and different types of modern methods to overcome the locking, all of them rely on some artificial stabilization techniques which deteriorate reliability. Nevertheless, there is a growing need for the multiscale (see Ghoniem 2003) and micro-macro approaches (see Schmauder 2002), it is still difficult to inflate atomistic models to the size of specimens and components.

In the present paper it will be shown that by use of the multifield reliable primal-mixed finite approach (see Mijuca 1997, 2004 and 2007) in thermo-mechanics, which has all variable of interest: temperature, heat flux, displacement and stress as solution variables, all above shortcomings are prevailed, and the introduced approach is both time efficient and adequate for straightforward coupling with nanomechanics. It is shown that the presented multiscale numerical approach, based on one-to-one correspondence between molecular dynamics (see Holian 1995) on atomistic scale and primal-mixed finite element scheme on macroscale, is reliable and efficient. The seamless semi-coupling between length scales can be achieved (Mijuca 2005). The reliability of the present primal-mixed FE approach is proved in Mijuca (2004) and (2007) for models in macroscale, and will be proved here for the multiscale model problems, from 0.01 micrometers upwards. It should be noted that different laws of physics are required to describe properties and processes of solids at different scales, so the author is of opinion that minimal geometric scales which we can now analyze, using the current physical laws, is 0.01 micrometers, and that is only because the approximation is performed by the reliable finite element.

We will use the following terminology in the present text. Geometrical *scale resolution* stands for the ratio between maximal axial dimension of the model problem and minimal axial dimension of finite elements, while *aspect ratio* stands for the ratio between maximal and minimal axial dimension of a finite element. In addition, the new definition should be stated: *Some numerical approximation procedure is multiscale reliable if it is reliable throughout the entire geometrical scale in which underlying physical law is valid.*

2. Primal-mixed formulation

We start from the special primal-mixed weak form in transient heat transfer, Mijuca (2007):

Find $\{T,q\} \in H^1(\Omega)\times H^1(\Omega)^n$ such that $T|_{\partial\Omega_T} = \overline{T}$ and:

$$\int_\Omega qk^{-1}Qd\Omega + \int_\Omega \nabla T\cdot Qd\Omega =$$

$$\int_\Omega \rho c\frac{\partial T}{\partial t}\theta d\Omega + \int_\Omega q\cdot\nabla\theta d\Omega - \int_\Omega \theta f d\Omega - \int_{\partial\Omega_q}\theta h d\partial\Omega - \int_{\partial\Omega_c} q_c\theta d\partial\Omega \tag{1}$$

for all $\{\theta,Q\} \in H^1(\Omega)\times H^1(\Omega)^n$ such that $\theta|_{\partial\Omega_T} = 0$.

The backward Euler scheme is used for the time discretization, where:

$$\rho c\frac{\partial T}{\partial t}\bigg|_n \approx \rho c\frac{{}^nT - {}^{n-1}T}{\Delta t} \tag{2}$$

For solving the behavior of the solid body under mechanical loading, Hellinger-Reissner's principle (Mijuca 2004), is used:

Find $\{\boldsymbol{u},\boldsymbol{t}\} \in H^1(\Omega)^n \times H^1(\Omega)^{n\times n}_{sym}$ such that $\boldsymbol{u}\big|_{\partial\Omega_t} = \boldsymbol{w}$ and:

$$\int_\Omega (\boldsymbol{A}\boldsymbol{t}:\boldsymbol{s} - \boldsymbol{s}:\nabla\boldsymbol{u} - \nabla\boldsymbol{v}:\boldsymbol{t})d\Omega = -\int_\Omega \boldsymbol{v}\cdot\boldsymbol{f}d\Omega - \int_{\partial\Omega_t}\boldsymbol{v}\cdot\boldsymbol{p}d\partial\Omega \tag{3}$$

for all $\{\boldsymbol{v},\boldsymbol{s}\} \in H^1(\Omega)^n \times H^1(\Omega)^{n\times n}_{\mathrm{sym}}$ such that $\boldsymbol{v}\big|_{\partial\Omega_t} = 0$

In the above expressions Ω is the domain of the solid body; T, $\boldsymbol{q}$, $\boldsymbol{u}$ and $\boldsymbol{t}$ are the temperature, heat flux, displacement and stress trial variables, respectively; while, θ, $\boldsymbol{Q}$, $\boldsymbol{v}$ and $\boldsymbol{s}$ are their test variables, respectively. The quantity $\boldsymbol{k}$ is a second order tensor of thermal conductivity, in general case, of an orthotropic material. If the material is homogeneous and isotropic, the tensor $\boldsymbol{k}$ will degenerate to a simple scalar value k, i.e. thermal conductivity. Further, ρ is the material density, and c is the specific heat, while f stands for the internal heat source generated per unit volume. Also, $\boldsymbol{A}$ is the fourth order compliance matrix tensor, $\boldsymbol{f}$ is the body force, and $\boldsymbol{p}$ is the vector of prescribed boundary tractions. Further, $H^1(\Omega)^{n\times n}_{sym}$ is the space of all symmetric tensorfields that are square integrable and have square integrable gradients, while $H^1(\Omega)^n$ is the space of all vectors that are square integrable and have square integrable gradients. The displacements and stresses are chosen from continuous subspaces, which is correct in the case of the homogeneous materials under mechanical loads. Nevertheless, on the surfaces of material discontinuities, only transversal stress component is continuous. It will be shown later in the text that this error is much smaller than in approaches where stresses are chosen from discontinuous subspaces $L^2(\Omega)^{n\times n}_{sym}$, as in the original version of Hellinger-Reissner's principle and *primal* approaches, see Arnold (1990).

It will be shown that the essential contribution of the present investigation is that the calculated temperatures are introduced directly in the field equation (3), i.e. without differentiation; this will be done through essential boundary conditions per stresses. We can see from (1) and (3) that temperatures and stresses are presently approximated by the functions of the same polynomial degree. This is because the constitutive equation between stress and thermal stress does not include the temperature derivative, hence there will be no *consistency error* between calculated thermal and stress deformation fields, see Prathap (1995).

It should be noted that the *consistency error* is a big shortcoming of the primal finite element approaches. In primal approaches, when temperatures and displacements are approximated by functions of the same polynomial degree, we found that polynomial degree of thermal strains is lower than the polynomial degree of mechanical strains. Namely, temperature enters the mechanical field equations ($[\mathbf{K}]\{\mathbf{u}\}=\{\mathbf{f}\}$) through the force loading term $\mathbf{f}$, by differentiation of thermal strains. So, the thermal strains will be in the polynomial function space that is one degree lower than mechanical space. It results in spurious oscillations of stresses, especially around singularities, as at corner nodes, reentrant nodes and material interfaces. In primal methods these oscillations can be avoided only if the polynomial degree of approximation function used for displacement is one order higher than for temperature.

In the case of traditional materials where there is no heat production due to strain rate, thermal effects on a body are limited to strains due to the temperature gradient, which are autonomously determined and constitute only a datum for stress analysis, see Cannarozzi (2001). Therefore, the strains are mechanical ($\boldsymbol{e}_p^M$) or thermal ($\boldsymbol{e}_p^T$), and they are additive in the linear case. On the other hand, in the present approach thermal strain will enter the formulation (3) as essential boundary condition per stress, using the constitutive equation. Namely, the corresponding prescribed thermal strains $\boldsymbol{e}_T^p$ are calculated from prescribed temperatures T_p using the following constitutive equation:

$$\boldsymbol{e}_T^p = \boldsymbol{\alpha}\left(T_p - T_i\right) \tag{4}$$

where $\boldsymbol{\alpha}$ is the second order tensor of thermal expansion coefficients (scalar in the case of isotropic materials), while T_i is the initial temperature. The prescribed thermal stresses $\boldsymbol{t}_T^p$ are then simply calculated from strains $\boldsymbol{e}_p^T$ via the constitutive relation:

$$\boldsymbol{t}_T^p = \boldsymbol{C} : \boldsymbol{e}_T^p \tag{5}$$

where, $\boldsymbol{C}$ is the elasticity matrix.

We can see from (1) and (3) that presently thermal stresses and mechanical stresses are calculated in the subspaces of the interpolation functions of the same degree without any loss in accuracy as in *primal* approaches. Therefore, we can say that the presented semi-coupling of thermal and mechanical physical problems is performed in the consistent way.

2.1 Finite element equations

As it is show in Mijuca (2007), the transient thermoelastic problem consists in determining the response of the body in terms of displacement $\boldsymbol{u}$, temperature T, stress $\boldsymbol{t}$ and heat flux $\boldsymbol{q}$, according to the compatibility equations, equilibrium and thermal balance equations, constitutive equations, and boundary and initial conditions:

$$\begin{bmatrix} \mathrm{A}_{vv} & \mathrm{-D}_{vv} \\ \mathrm{-D}_{vv}{}^{T} & 0 \end{bmatrix} \begin{bmatrix} \mathrm{t}_v \\ \mathrm{u}_v \end{bmatrix} = \begin{bmatrix} \mathrm{-A}_{vp} & \mathrm{D}_{vp} \\ \mathrm{D}_{pv}{}^{T} & 0 \end{bmatrix} \begin{bmatrix} \mathrm{t}_p \\ \mathrm{u}_p \end{bmatrix} - \begin{bmatrix} 0 \\ \mathrm{f}_p + \mathrm{p}_p \end{bmatrix} \tag{6}$$

$$\begin{bmatrix} \mathrm{M}_{vv} & \mathrm{B}_{vv}{}^{T} \\ \mathrm{B}_{vv} & -\mathrm{D}_{vv} - \mathrm{S}_{vv} \end{bmatrix} \begin{bmatrix} \mathrm{q}_v \\ \mathrm{T}_v \end{bmatrix} = \begin{bmatrix} -\mathrm{M}_{vp} & -\mathrm{B}_{vp}{}^{T} \\ -\mathrm{B}_{vp} & \mathrm{D}_{vp} \end{bmatrix} \begin{bmatrix} \mathrm{q}_p \\ \mathrm{T}_p \end{bmatrix} + \begin{bmatrix} 0 & 0 \\ 0 & \mathrm{S}_{vp} \end{bmatrix} \begin{bmatrix} 0 \\ \mathrm{T}_p^{(t-1)} \end{bmatrix} + \begin{bmatrix} 0 \\ \mathrm{F}_p + \mathrm{H}_p - \mathrm{K}_p \end{bmatrix} + \begin{bmatrix} 0 \\ -\mathrm{L}_p^{(t-1)} \end{bmatrix} \tag{7}$$

where,

$$\begin{aligned} A_{\Lambda u v \Gamma s t} &= \sum_e \int_{\Omega_i} \Omega_\Lambda^N S_N g^a_{(\Lambda)u} g^b_{(\Lambda)v} A_{abcd} g^c_{(\Gamma)s} g^d_{(\Gamma)t} T_L \Omega_\Gamma^L d\Omega \\ D^{\Gamma q}_{\Lambda u v} &= \sum_e \int_{\Omega_\blacklozenge} \Omega_\Lambda^N S_N U_a^K \Omega_K^\Gamma g^a_{(\Lambda)u}\ g^{(\Gamma)q}_{(\Lambda)v} d\Omega \\ f^{\Lambda q} &= \sum_e \int_{\Omega_\blacklozenge} g_a^{(\Lambda)q} \Omega_M^\Lambda V^M f^a d\Omega \\ p^{\Lambda q} &= \sum_e \int_{\partial\Omega_{it}} g_a^{(\Lambda)q} \Omega_M^\Lambda V^M p^a d\partial\Omega \end{aligned} \tag{8}$$

and

$$
\begin{aligned}
M_{\Lambda p\Gamma r} &= \sum_{\Omega_\varepsilon} \int \overset{(e)}{\Omega^L_\Lambda} g^a_{(L)p} V_L k^{-1}_{ab} g^b_{(M)r} V_M \, \overset{(e)}{\Omega^M_\Gamma} d\Omega_e \\
B_{\Lambda p\Gamma} &= \sum_e \int_{\Omega_e} \overset{(e)}{\Omega^L_\Lambda} \, g^a_{(L)p} V_L P_{M,a} \, \overset{(e)}{\Omega^M_\Gamma} d\Omega_e \\
D_{\Lambda\Gamma} &= \sum_e \int_{\partial\Omega_{ce}} h_c \, \overset{(e)}{\Omega^L_\Lambda} P_L P_M \, \overset{(e)}{Q^M_\Gamma} \partial\Omega_{ce} \\
S_{\Lambda\Gamma} &= \sum_e \int_{\Omega_e} \frac{\rho c}{\Delta t} \overset{(e)}{\Omega^L_\Lambda} P_L P_M \, \overset{(e)}{\Omega^M_\Gamma} d\Omega_e \\
L_\Gamma &= \sum_e \int_{\Omega_e} \frac{\rho c}{\Delta t}^{n-1} T_{(M)} P_M \, \overset{(e)}{\Omega^M_\Gamma} \, d\Omega_e \\
F_\Gamma &= \sum_e \int_{\Omega_e} \overset{(e)}{\Omega^M_\Gamma} P_M f d\Omega_e, H_\Gamma = \sum_e \int_{\partial\Omega_{he}} \overset{(e)}{\Omega^M_\Gamma} P_M h d\partial\Omega_{he} \\
K_\Gamma &= \sum_e \int_{\partial\Omega_{ce}} \overset{(e)}{\Omega^M_\Gamma} P_M h_c T_a d\partial\Omega_{ce}
\end{aligned}
\tag{9}
$$

It is obvious from (1) and (3) that present primal-mixed finite element approaches represent a saddle point problem, where system matrix is indefinite with additional sparsity concerning zero-diagonal entries. Solvers MA57 and MA47 from Harwell Subroutine Library, which are designed for the solution of this kind of systems, are chosen as suitable for testing. They are based on the multifrontal method which is a direct approach for solving linear systems of equations. Like most sparse direct solvers, algorithms are developed in three distinct computational phases: analyze, factorize and solve phase, Duff (1986).

3. Dimensional reduction

Dimensional reduction is one of the two generic techniques for model idealization, see Babuska. (1991). The solid bodies with one or two axial dimensions much smaller than other are traditionally examined by plate, shell or beam theories based on dimensional and solution variable reduction in the direction normal to middle surface, or beam's cross section, respectively. Obviously, these geometrical simplifications produce errors in the final solution, which are traditionally considered to be negligible. From the historical point of view, plate, shell and beam theories were needed to enable simplified engineering calculations. On the other hand, in order to capture stress concentrations at local details, it is often desirable to combine the reduced dimensional element types with higher dimensional elements, like hexahedral, in the entire global model. Consequently, it is necessary to have some scheme for coupling the element types that conforms to the governing equations of the problem, and which do not introduce any spurious results of dual variable (stress, heat flux) at the dimensional interface. However, regardless of the coupling technique, there will be some so-called transition error introduced.

Theories based on the dimensional reduction suffer from the aspect-ratio restriction, which is highly inappropriate in multiscale analysis, where the atomistic region is bridged to a

continuum region and therefore very narrow finite elements are welcomed. In addition, the existing theories are inappropriate in analyses of coated bodies or thin films of micron sized and less.

Nevertheless, idealization of geometry in order to reduce the complexity of the model is the major factor limiting the wider application of FEA in computational materials technology where the material is respected throughout the dimensional scales. In addition, in the case when finite element approach is primal, model problem is approximated by plates or shells, and the material undergoes plastic deformation or applied external loading produces excessive bending, so that the system matrix will become highly ill-conditioned.

4. Multiscale robustness

There is a growing need to develop systematic modeling and simulation approaches for multiscale multimaterials model problems to provide the accurate data about the state of stress, defect structure, thermal and mechanical performance of subregions with different geometric scales. These problems arise, for example, in the analysis of coated components, where materials scientist use soft, hard, biomimetic, wear resistant or corrosion protecting multiphase or multilayer coatings to gain significant performance advantages (e.g. thermal coating of metal based turbines with some ceramics). The other example is a multi-layered microelectronic packaging or wind turbine, where the interfacial stress induced by thermal loading or moisture during manufacturing or exploitation is responsible for delamination-related failures. Reliability of the present FE HC8/27 makes it a candidate of the first choice for the use in thermo-mechanical multiscale analysis, such as aforementioned examples where high aspect ratio of the FEs is inevitable.

5. The mathematical convergence requirements

As the finite element mesh is refined, the solution of the discrete problem should approach to the analytical solution of the mathematical model, i.e. to converge. The convergence requirements for shape functions of isoparimetric elements are grouped into three categories, i.e: completeness, compatibility and stability, see Arnold (1990) and Rannacher (1997). In addition, the consistency and stability imply convergence. If the stability condition is satisfied, there will be no non-physical zero-energy modes (kinematic modes).

The *completeness* criterion requires that elements must have enough approximation power to capture the analytical solution in the limit of a mesh refinement process. Therefore, the approximation functions must be of certain polynomial order that ensures that all integrals in the corresponding weak formulation are finite. Further, the *compatibility* requirement demands that shape functions provide displacement continuity between elements. Then, it will be ensured that no artificial material gaps will appear during the deformation of finite element mesh. As the mesh is refined, such gaps could multiply and may absorb or release spurious energy.

Completeness and compatibility are the two aspects of the so-called *consistency* condition between the discrete and mathematical models. A finite element model that passes both completeness and continuity requirements is called *consistent.*

Further, if the method is *stable*, the non-physical zero-energy modes (kinematic modes) in finite element model problem will be prevented. The kinematic modes are extra zero-eingenvalues of a finite element system matrix. The finite element is stable if it satisfies

two necessary conditions: the first one is represented by the *ellipticity on the kernel* condition, and second is represented by the *inf-sup* condition (Bathe 19976).

It should be noted that satisfaction of the completeness criterion is necessary for the convergence, while violating the other two criteria does not necessarily mean that the solution will not converge. However, if the method is not stable, at least what could happen is that approximate solution will not converge to the analytical solution at the same rate as the best approximation error. Hence, in the best scenario the approximate solution will slowly converge to the analytical solution of the mathematical model. In the worst scenario, the system matrix will be singular, thus without solution of the given model problem at all.

5.1 Consistency condition

In the presented formulation, the *completeness* requirement is satisfied as the local approximation finite element functions poses all polynomial terms of degree $k=3$, needed for the present three-dimensional case. Further, both finite approximation subspaces of stress and displacements are from space H^1 over the domain of the model problem. Consequently, it is provided that these spaces are continuous over an interelement boundary, resulting that the compatibility requirement is also satisfied.

5.2 Reliability of the finite elements

The overall stability of the mixed formulations based on Hellinger-Reissner's principle is provided if two necessary conditions for stability are fulfilled i.e., the first stability condition represented by the ellipticity on the kernel condition, and second stability condition represented by the so-called *inf-sup* condition, Arnold (1990). The second stability condition is very hard to be satisfied. However, the satisfaction of the inf-sup condition ensures solvability and optimality of the finite element solution, and it is very important to be satisfied if the finite element approach is to be used for the complex model problems.

5.3 First stability condition

The *ellipticity on the kernel* condition is given by:

$$a(z,z)\le \alpha_h \|z\| \text{ for all } z\in Z_h,\ Z_h=\left\{z\in S_h \,\middle|\, b(z,\boldsymbol{v})=0 \text{ far all } \boldsymbol{v}\in V_h\right\} \tag{10}$$

Spaces S_h and V_h are the finite dimensional subspaces of test stress spaces $\boldsymbol{S}$ and displacement spaces $\boldsymbol{v}$, respectively.

In the presented formulation, the test and trial stress local functions are from spaces $S_h\subset\left(H^1\right)^{n\times n}$. Therefore, the corresponding bilinear form a in (3) is quadratic. In addition, in the physical sense it represents the deformation energy, which is positive definite for linear elasticity problems. Consequently, it is also symmetric and bounded. From all these properties of the given bilinear form a, we can conclude that the first stability condition is automatically satisfied.

5.4 Second stability condition

The second stability condition is satisfied if the value γ_h, following from LBB (Ladyzhenskaya, Babuška, Brezzi) condition (see Brezzi 1991, p.76, Eq.(3.22)), remains bounded above zero for the meshes of increasing density:

$$\gamma \le \gamma_h = \inf_{\boldsymbol{v}\in V_h} \sup_{\boldsymbol{s}\in S_h} \frac{b(\boldsymbol{S},\boldsymbol{v})}{\|\boldsymbol{S}\|\|\boldsymbol{v}\|} \tag{11}$$

Since the verification of the condition like (11) involves an infinite number of meshes, a numerical inf-sup test should be performed for a sequence of several meshes of increasing refinement. For the presented choice of approximation spaces V_h and S_h, the above condition can be read as:

$$\gamma \le \gamma_h = \inf_{\boldsymbol{v}\in H^{1(n)}} \sup_{\boldsymbol{S}\in H^{1(n\times n)}} \frac{b(\boldsymbol{S}_h,\boldsymbol{v}_h)}{\|\boldsymbol{S}_h\| \ \|\boldsymbol{v}_h\|} \tag{12}$$

where,

$$b(\boldsymbol{S}_h,\boldsymbol{v}_h) = \sum_e \int_{\Omega_i} \boldsymbol{S}_h : \nabla \boldsymbol{v}_h d\Omega_e \tag{13}$$

$$\|\boldsymbol{S}_h\|^2 = \sum_e \int_{\Omega_i} \boldsymbol{S}_h : \boldsymbol{S}_h d\Omega_e \tag{14}$$

$$\|\boldsymbol{v}_h\|^2 = \sum_e \int_{\Omega_i} \nabla \boldsymbol{v}_h{}^{\mathrm{T}} : \nabla \boldsymbol{v}_h d\Omega_e \tag{15}$$

In addition, the condition (11) ensures solvability and optimality of the finite element solution (see Arnold 1990). It is interesting to note that any loading does not enter the test. It should be noted that the discrete LBB condition in the present formulation is equivalent to the statement that for each $\boldsymbol{v} \in V_h$ there is an i such that:

$$\nabla \boldsymbol{v}_h \in (S_h)_i \tag{16}$$

There are only several finite elements which satisfy this condition in the known literature. Moreover, this condition is dependent on the number of finite elements in the mesh (mesh size). Consequently, numerical inf-sup test is represented by the generalized eigenvalue problem, in matrix notation given by:

$$\mathbf{D}_h^{\mathrm{T}} \mathbf{A}^{-1} \mathbf{D}_h \boldsymbol{x} = \lambda \mathbf{C}_h \boldsymbol{x} \tag{17}$$

where $\mathbf{D}$ and $\mathbf{A}$ are matrix entries in (6). And matrix $\mathbf{C}$ is the stiffness matrix from the corresponding displacement based (primal) finite element method, given by:

$$K^{\Lambda m \Gamma n} = \sum_e \Omega_L^{\Lambda} \int_{\Omega_i} g_a^{(\Lambda)m} U_b^L C^{abcd} U_d^K g_c^{(\Gamma)n} d\Omega \, \Omega_K^{\Gamma} \tag{19}$$

The square root of the smallest eigenvalue of the above problem $\sqrt{\lambda_{\min}}$ is equal to the inf-sup value γ_h in equation (12). The test involves, following Bathe (1996), the determination of γ_h for several meshes with increasing refinement with the mesh density indicator $1/N$, via calculation of $\lambda_{\min}$.

If the inf-sup values, for a chosen sequence of finite element meshes, do not show a decrease toward zero, meaning that the $\gamma = \sqrt{\lambda_{\min}}$ values stabilize at some positive level, then it can be considered that the inf-sup test is passed. It should be noted that decreasing of the inf-

sup values on log-log diagram would be seen as a curve with moderate or excessive slope. This approach is used in Mijuca (2004) and (2007) to test stability of the present finite element in the non multiscale analysis. It was shown that the present FE satisfies all these criteria in geometrically non-multiscale analysis, for both, regular and extremely distorted finite element meshes, and for compressible and nearly incompressible materials. The first stability condition is *a priori* satisfied for the present FE formulation, and it is also the mesh size undependable. Therefore, in order to prove the reliability of the present FE HC8/27 in geometrically multiscale analysis, we will have to prove only the second stability condition. The results of the inf-sup test for the present finite element configuration HC8/27 are given in the next section.

6. Numerical examples

Several model problems from thermo-mechanics with geometrical *scale resolution* up to 8 orders of magnitude, and *aspect ratio* up to 7 orders of magnitude, are presently investigated (for terminology see Section 1). They are used to test reliability, time efficiency and accuracy of the present primal-mixed finite element approach HC8/27. The performance with respect to scaling is highlighted. Model problems with high aspect ratio, highly distorted hexahedral finite elements, multimaterial model problems, as bimetallic strip and thermally coated shaft, and inf-sup test on multiscale regular, highly distorted, compressible and incompressible unit brick, are performed in the next examples..

The results are, where appropriate, compared with the primal hexahedral finite element H8 and analytical solutions, as in Roark (1975). The finite element H8 is based on the primal finite element approach, namely, *displacement finite element method* with incompatible displacement modes (so-called bubble modes) introduced into the element (see Wilson 1990), which are eventually eliminated from the element stiffness matrix by the static condensation procedure. A special integration scheme is used to ensure that H8 passes the patch test, while the stress field is obtained *a posteriori* and smoothed by the local stress averaging.

6.1 Inf-sup test in multiscale analysis of the unit brick

The inf-sup test (second stability condition) of the present finite element HC8/27 in the geometrically multiscale analysis is checked on the model problem of the unit brick following Bathe (1996), with regular or extremely distorted finite element meshing, and for aspect ratio of finite elements up to 6 orders of magnitude, and scale resolution of model problem up to 7 orders of magnitude.

The Young modulus is 1 and Poisson's coefficient is 0.3 for compressible, and 0.49 for nearly incompressible materials. The unit brick is discretized by sequence of the finite element meshes with pattern $N\times 2\times 2$, where $N=1,2,3,4,6$, along x, y and z axes. The first section per x axis is 0.999999 thick, and the second section per x axis is 0.000001 thick. Therefore, in undistorted mesh for the $N=6$, the minimal axial dimension of FE is $h_{\min}=1.66\cdot 10^{-7}$. The maximal axial dimension of the FE for all problems is $h_{\max}=0.5$, so the aspect ratio is $h_{\max}/h_{\min}=3\cdot 10^{6}$, that is, more than 6 order of magnitude. In that case the scale resolution is $1/h_{\min}=1.66\cdot 10^{7}$, that is seven orders of magnitude. For extremely distorted meshes, the midside points are moved from $M\left(x,0.5,0.5\right)$ positions, to $M\left(x,0.7,0.7\right)$, and maximal aspect ratio is $h_{\max}/h_{\min}=4.4\cdot 10^{6}$ (see Figure 1). The results are plotted in the form

$\log(\gamma_{\min}) = f(1/N)$, where $\gamma_{\min} = \sqrt{\lambda_{\min}}$ is the square root of minimal eigenvalue in (13). Results are plotted from right to left for meshes of increasing refinement in Figure 2.

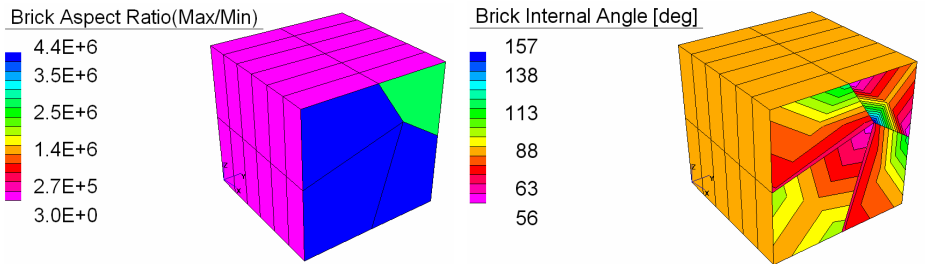

Fig. 1. Maximal aspect ratio and internal angle for the unit brick model problem.

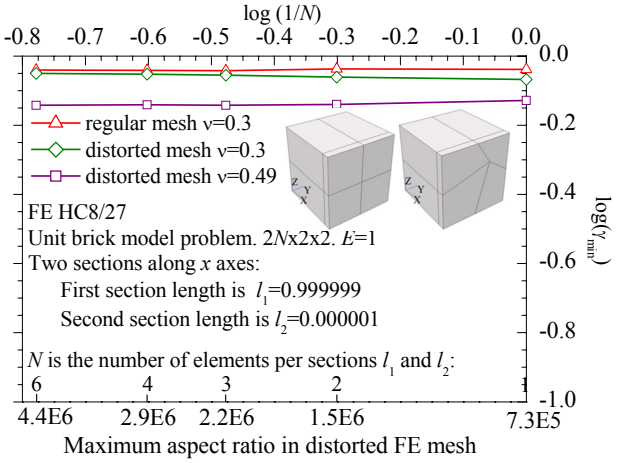

Fig. 2. Inf-sup reliability test: Unit brick model problem.

We can see from Figure 2, that regardless of the aspect ratio and mesh pattern N, the inf-sup curves of finite element HC8/27 do not show decrease toward zero, but remains stabilized at some level. Therefore, we may conclude that the finite element HC8/27 passes the inf-sup test in compressible and nearly incompressible cases, for regular and extremely distorted finite elements in the mesh, where the aspect ratio of minimal and maximal axial dimensions of the finite elements is up to $3 \cdot 10^6$. The inf-sup test results of the other sub-configurations of present FE will be given in a separate paper.

Keeping in mind that it is already proved in Mijuca (2007) that the present finite element passes the first stability condition (which is *a priori* satisfied), and that it satisfies the c*ompleteness* criterion and *compatibility* criterion, we may say that the present finite element is reliable under definition set in Section 1.

6.2 Long steel coated shaft

The simulation of coated materials is of particular interest to industry in order to control the level of the interfacial stresses on the surfaces of material discontinuities, see Lu (2003). Therefore, a hollow shaft covered with microsized coating layer for mechanical and thermal protection, shown in Figure 3, is presently examined.

The material properties are given in Table 1. The inner and outer radii of the shaft are $0.005m$ and $0.1m$, respectively. The coating consists of a bond and ceramic layers of the equal size. Thickness of the coating (bond and ceramic) is gradually decreased from $h=10^{-2}m$ to $h=10^{-6}m$, in order to check robustness of present finite element to high distortion. The reference temperature is $T_R=1273K$. The shaft is loaded by prescribed temperatures on inner and outer surfaces, such that $T_i=773K$ and $T_o=1273K$, respectively. It is assumed that height off the shaft is $0.1m$. Consequently, on material interfaces all stress tensor components, except radial, will be discontinuous and will differ significantly due to the large difference in physical properties of the bonded materials. The target solution of radial stress is obtained by a modified plate theory. We will investigate the convergence of the temperature and radial stress component on the interface L2, between bond and ceramics, for the sequence of five model problems with decreasing coating thickness $h=10^{-N}$, where $N=2,3,4,5,6$.

Long steel coated shaft - material properties					
	Modulus	Poisson's ratio	Thermal expansion coefficient	Density	Thermal conductivity
	$E\cdot 10^4\left[MPa\right]$	ν	$\alpha\cdot 10^{-5}\left[{}^0/C\right]$	$\rho\cdot 10^3\left[kg\right]$	$k\left[W/m^2C\right]$
Ceramic	1.0	0.25	1.0	4.0	1
Bond	13.7	0.27	1.51	4.0	25
Steel	21.0	0.30	2.0	7.98	25

Table 1. Long steel coated shaft - material properties.

Only one-quarter of the model problem is analyzed due to the symmetry. Both bond and ceramic are discretized by 3 layers of finite elements along the radius. The model problem is plain strain, so only one finite-element layer along its height is presently used. Consequently, for the last model problem, where coating is thick $h=10^{-6}m$, we will have the maximum finite element aspect ratio equal to 600000. The temperature distribution is calculated by present thermal approach (6), after which the thermal stresses are calculated by (8) without the *consistency* error.

The results obtained by the present finite element HC8/9 and classical plane boundary element method (CBEM), see Lu (2003), for temperature and stress at the interface r_1, are shown in Figures 3 and 4, respectively. We may see that the approach CBEM exhibits spurious oscillation of results. On the other hand, the present approach results are invariant to the size coating thickness. In addition, the convergence is achieved.

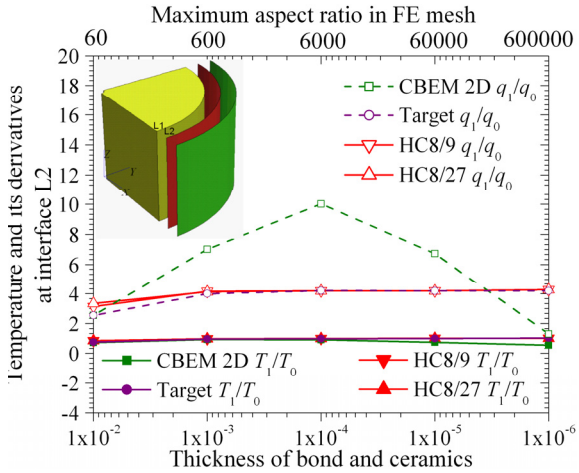

Fig. 3. Coated shaft. Convergence of temperature results at boundary L2.

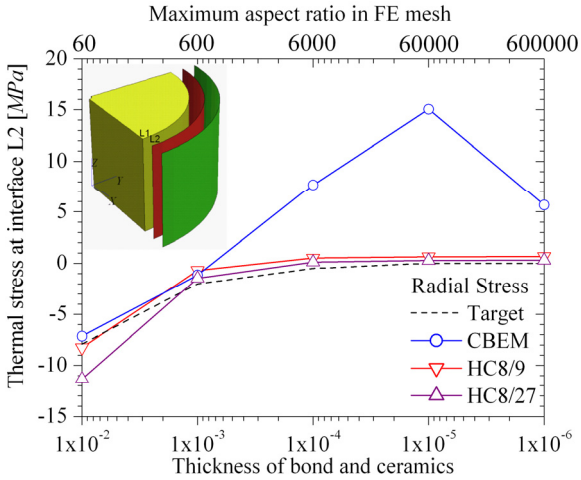

Fig. 4. Coated shaft. Convergence of thermal stress results at boundary L2

We now investigate the convergence of the stress in x-direction around the surfaces of material discontinuities on L1 and L2, for model problem $t = 10^{-6} m$, are shown in Figure 5, where we can notice that there are no spurious oscillations of the stresses.

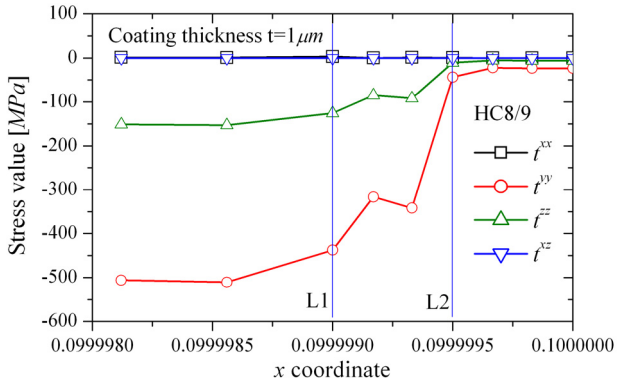

Fig. 5. Coated shaft. Model problem with coating thickness $t = 1\mu m$. Stress along x axis.

The execution time for the three distinct phases in the solution process, the storage requirements, and backward error for the in-house direct Gaussian solver and MA57 solver with scaling routine MC64, are reported in Table 2. Numerical experiments were conducted on a PC Pentium(R) D CPU 2.8 GHz with 3.25GB of RAM with Physical Address Extension running under the operating system Microsoft Windows XP Professional Version 2002 Service Pack 2, double precision (64-bit) reals were used, and CPU times are given in seconds.

Coated cylindrical shaft - execution time and storage requirements								
				Time				Backward
	FE	N	NE	Analyze	Factorize	Solve	Total	error
in-house	HC8/9	5776		14.31		.75	15.06	
	HC20/21	16500		1810.17		4.89	1815.06	
MA57 + MC64	HC8/9	5776	280056	.03	.50	.01	.54	.8E-12
	HC20/21	16500	1829790	.17	12.28	.05	12.50	.1E-10
	HC8/27	18634	1961070	.19	4.05	.06	4.30	.2E-10
	HC20/27	22122	2785700	.27	11.59	.08	11.94	.3E-10

Table 2. Coated cylindrical shaft - execution time and storage requirements.

We can see from results reported in Table 2 that scaling the system matrix prior to the factorization using MC64 routines considerably improves the execution time. In addition, the storage requirements and number of operations are far smaller. The MA57 without scaling was not able to solve some model problems, because the factorization fails due to insufficient storage. Therefore, the conclusion is that scaling generally decreases the storage requirements, decrease the solution time, and handles the solution of systems with much more degrees of freedom. As an interesting aside to this set of problems, the given matrix has many entries of very small size (around 10^{-20}). However, these are significant numbers inasmuch if they are treated as zero, and it is not possible to solve the resulting systems because the matrix is singular.

6.3 Bimetallic strip

Bimetallic strips are widely used in instruments to sense a control temperature. They are made up of two or more metallic layers having different coefficients of expansion, causing the material to change its curvature when subjected to a change in temperature (see Roark 1975).

The cantilever bimetallic strip of length $l = 10$, width $w = 0.1$, and thickness $t = 0.1$, is considered in the present example. The goal is to check if there is spurious stress beahaviour from singularity of stress on the clamped edge and material interface. Finite elements HC8/9, HC8/27 and HC20/21, are investigated. The results are compared with results obtained by primal finite element method based on displacement based approach, finite elements H8 and H20, with local stress averaging. It should be noted that we are aware that primal finite elements are not designed to be used in multiscale resolution model problems, due to the hourglass locking. Nevertheless, it will help us to emphasize the robustness of present finite elements.

The beam is stress free at $T_R = 70$ and subjected to a uniform temperature $T_0 = 170$. Both materials have modulus of elasticity $E = 3 \cdot 10^7$ *MPa* and Poisson's ratio $\nu = 0.3$. The only difference is in coefficients of thermal expansion, which are $\alpha_1 = 1 \cdot 10^{-5}$ and $\alpha_2 = 2 \cdot 10^{-5}$, for the upper and lower material, respectively. Consequently, all components of stresses at the material interface, except transversal, will be singular. We assume that the beam longitudinal axe coincides with the x direction. Nodes on the clamped edge have suppressed displacements. Analytical solutions, obtained by the modified simple beam theory (see Roark (1975), page 114) is $t^{xx} = -7500$, for the top surface, and maximal deflection is $u_z = 0.75$. Only one half of the model problem is analyzed due to the symmetry.

Present model problem has one material surfaces of discontinuity on the interface between two materials, and one line of discontinuity on the clamped edge. In order to localize the stress singularity on the material interface, we place a very thin layer of finite elements on the both sides of the material interface, one layer on each side, with thickness $h_b = 0.0001m$. Further, we localize the effect of stress singularity on the clamped edge by placing one or several microsized finite elements near the clamped edge with thickness $h_c = 0.000001m/N$. Therefore, we are expecting convergence of displacements at the clamped edge, but do not expect the convergence of the stress at midsection node of the beam, as maximal stress of the model problem is at the clamped edge and it is singular. The mesh pattern is given by $(10N + N) \times 1 \times (2 + 1 + 1 + 2)$, for $N = 2, 4, 8, 16$. Namely, in order to localize singularity of stress at the clamped edge, N layers of finite elements with thicknesses $h = 0.0001/N$ just adjacent to the clamped edge, are generated.

Consequently, the *scale resolution*, i.e. the ratio of maximal axial dimension of the model problem ($l_{\max} = 10m$) and minimal axial dimension of finite elements ($h_{\min} = 0.000001/16 = 6.25 \cdot 10^{-8}$), is $l_{\max}/h_{\min} = 1.6 \cdot 10^8$ (up to 8 orders of magnitude). Maximal *aspect ratio* of finite elements in the present model problem is $h_{\max}/h_{\min} = 1 \cdot 10^7$, i.e. 7 orders of magnitude. Convergences of the target values using finite elements HC8/9, HC8/27 and HC20/21, are given in Table 3.

Convergence of maximal displacement u^z

Mesh pattern $(10N+N)\times 1\times 4$. Thickness of the bond layers $h_b = 0.0001m$.

Thickness of the layers near the clamped edge $h_c = 0.000001m/N$.

Aspect ratio $h_{\max}/h_{\min} = 1\cdot 10^6$, for $N = 2,4,8,16$

N	NEL	Scale resolution $l_{\max}/h_{\min}$	HC8/9	HC20/21	HC8/27	H8	H20
2	88	2E+07	.6649954	.7500676	.5861077	0.7500546	0.7501663
4	176	4E+07	.7311053	.7500674	.7131315	0.7500688	0.7499819
8	352	8E+07	.7464689	.7500664	.7430614	0.7500615	0.7501227
16	704	11.6E+08	.7495121	.7500637	.7490083	0.7500665	0.7505277

$u_z = 0.75$; $t^{xx}_{\text{target}} = 7500$

Table 3. Cantilever bimetallic strip. Convergence of maximal displacement u^z.

It can be seen from Table 7 that all three types of considered finite elements, uniformly converges to the analytical displacement, while the finite elements H8 and H20 oscillate around analytical solution.

We now investigate variation of target stress t^{xx} along the upper line $(x, 0.05, 0.05)$. The results for linear finite elements: primal H8 and primal-mixed HC8/27, are shown in Figure 6. We can see that the present configuration HC8/27 does not exhibit spurious oscillations. Note that this finite element passes inf-sup test (see Example 6.1).

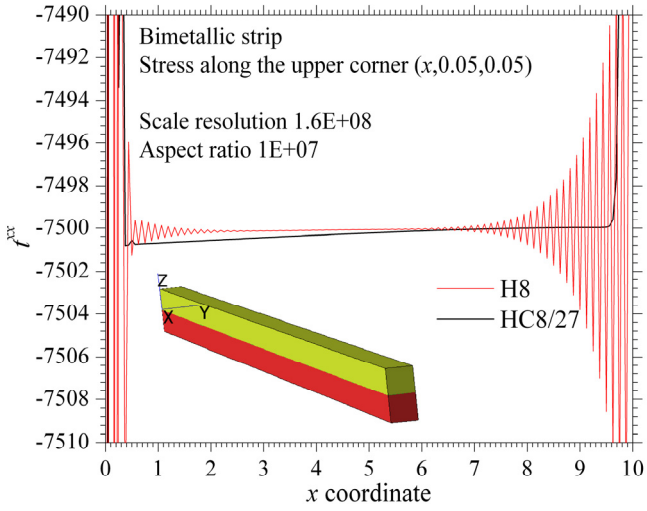

Fig. 6. Bimetallic strip. stress t^{xx}. Primal H8 and primal-mixed HC8/27 finite element.

6.4 Hollow sphere with two materials and convective BC's

Sensitivity of the present approach to the presence of the material discontinuity is investigated in this example. A model problem is the steady state heat transfer through a hollow bimaterial sphere (see Societe Francais, 1989). Inner, interfacial and outer radius of the hollow sphere are $0.3m$, $0.35m$, and $0.37m$, respectively. The convection boundary conditions are prescribed on

its inner and outer surface, such that $h_c^{\text{inner}} = 200\, W/m^{2\,\circ}C$ and $T_a^{\text{inner}} = 70^0 C$, and $h_c^{\text{outer}} = 150\, W/m^{2\,\circ}C$ and $T_a^{\text{outer}} = -9^0 C$, respectively. Thermal conductivities of the inner and outer material are $k^{\text{inner}} = 40 W/m^{2\,0}C$ and $k^{\text{outer}} = 20\, W/m^{\circ}C$. The target values are temperatures on three characteristic radii: inner, interfacial and outer, which are $T_{\text{A}} = 25.06^0 C$, $T_{\text{B}} = 17.84^0 C$ and $T_{\text{C}} = 13.16^0 C$, respectively.

Only one-eighth of the hollow sphere is presently analyzed due to symmetry. The finite element configurations used were HC8/9, HC8/15, HC8/27, HC20/21 and HC20/27, and the raw primal one H8. The sequence of models with uniform meshes refinement in all directions were investigated. Relative errors of the calculated temperatures on characteristic radii at point B vs. the number of finite elements in the mesh, are shown in Figure 7. The obtained results reveal that all considered finite element configurations have high accuracy. In addition, artificially enforced continuity of heat flux shape functions along discontinuity surface of the abrupt material change (Point B) does not deteriorate results. Nevertheless, the quadratic finite element configurations H20, H20/21 and H20/27 have relative error less than 0.01% immediately after the second discretization, which points out very high accuracy of these configurations. It can be seen that very good results are obtained even with small number of elements in radial direction.

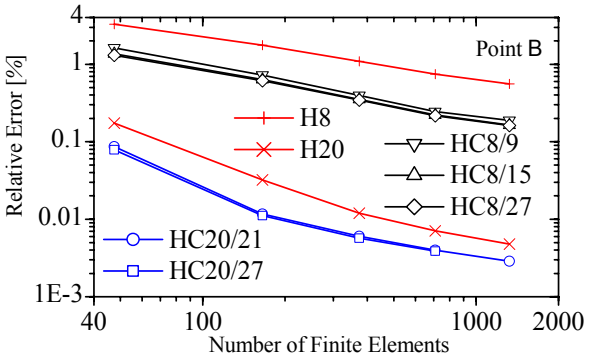

Fig. 7. Hollow sphere - uniform refinement: relative errors.

7. Conclusion

The geometrical scale resolutions up to 8 orders of magnitude and aspect ratio of finite elements up to 7 orders of magnitude are considered, using reliable and time efficient three-dimensional multifield primal-mixed hexahedral finite element approach in thermoelastic geometrically multiscale analysis in multi material solid mechanics, based on Hellinger-Reissner's principle. It has several essential contributions in accordance to other finite element approaches. Firstly, stress and heat flux are the solution variables as displacement and temperature, respectively. Therefore, stress constraints can be introduced as essential boundary conditions and any stress components can be set free or suppressed. For example, if we want to simulate beam or plate theory we can suppress transversal normal and shear stress components. In order to avoid the geometrical invariance error and to enable the introduction of displacement and stress constraints in an adequate coordinate system, the underlying finite element scheme is coordinate independent. Secondly, the approach is invariant to distortion and aspect ratio of finite elements. Namely, aspect ratio of hexahedral finite elements in the mesh could be up to 6

orders of magnitude, while they are degenerated to tetrahedron and L like shapes, without compromising the convergence.

In multimaterial bodies microsized finite elements are placed adjacent to surfaces of the material discontinuities, in order to localize singularity. Furthermore, nearly incompressible materials are analyzed without volumetric locking, without spurious oscillations of results near singularity. In addition, as stress is the solution variable, initial stress and/or strain field is introduced directly. This last feature is presently used in an original consistent approach for calculation of thermal stresses. The new definition of multiscale reliability is given. It is proved that proposed finite element HC8/27 passes the *inf-sup test* in a multiscale analysis, for geometrically highly distorted multiscale mesh, where the aspect ratio of finite elements and scale resolution of model problems are 6 and 7 orders of magnitude, for compressible and nearly incompressible materials and for thin solid bodies, respectively. Therefore, the present procedure is ready to be bridged with simulation approaches on particle levels.

From a number of benchmark tests performed, we can see that present approach provides accurate results, with an execution time which is at least three orders of magnitude shorter than the elsewhere reported results. Further, it is shown that the dimensional reduction or neglecting some stress components, usual in beam and plate theories, can lead to the substantial underestimation of thermal stresses, which is already noticed in experimental testing. In addition, it is shown that the primal finite element approach under dimensional reduction theories underestimate maximal thermal stresses. Consequently, the satisfaction of the convergence requirements of the present finite element scheme makes it a promising field for future research undertakings, including developments in materially non-linear solid continua, or in coupling with other physical fields, as fluid or electro-magnetic.

Acknowledgements

My special thanks go to Iain Duff elected Fellow of the Royal Society of Edinburgh, for his collaboration in implementation of solver MA57 and scaling routine MC64 in present approach. The work on present text was supported by the Ministry of Science of Republic of Serbia grant 144007.

References:

Arnold DN. Mixed finite element methods for elliptic problems, Computer Methods in Applied Mechanics and Engineering, 82, 1990, pp.281-300

Babuska I. On a dimensional reduction method. III, A-posteriori error estimation and an adaptive approach, Math. Comp., 37, 156, 1981, pp. 361-383 (with M. Vogelius),

Bathe KJ. On reliability in the simulation of structural and fluid flow response. Advances in Computational Methods for Simulation. Civil-Comp Press, Edinburgh, 1996, pp. 1-7

Brezzi F, Fortin M. Mixed and Hybrid Finite Element Methods, Springer-Verlag, New York. 1991

Cannarozzi AA, Ubertini F. A mixed variational method for linear coupled thermoelastic analysis. International Journal of Solids and Structures 38, 2001, pp. 717-739

Chavan KS, Lamichhane BP, Wohlmuth BI. Locking-free finite element methods for linear and nonlinear elasticity in 2D and 3D. Computer Methods in Applied Mechanics and Engineering. 196 (41), 2007, pp. 4075-4086

Duff IS, Erisman AM, Reid JK. Direct methods for sparse matrices. Oxford University Press, London, 1986

Duff IS, Reid JK. The multifrontal solution of indefinite sparse symmetric linear systems, ACM Transactions on Mathematical Software 9, 1983, pp.302–325

Ghoniem NM, Busso EP, Kioussis N, Huang H. Multiscale modelling of nanomechanics and micromechanics: an overview. Philosophical Magazine, 1 Nov–1 Dec 2003, Vol. 83, Nos. 31–34, pp. 3475–3528

Holian BL, Voter AF, and Ravelo R. Thermostatted molecular dynamics: How to avoid the Toda daemon hidden in Nose-Hoover dynamics, Physical Review E 52 (3): 1995, pp.2338-2347.

Icardi U. Layerwise mixed element with sublaminates approximation and 3D zig-zag field, for analysis of local effects in laminated and sandwich composites. International Journal for Numerical Methods in Engineering. on line first, 2006

Djoko J, Lamichhane B, Reddy D, Wohlmuth B. Conditions for Equivalence between the Hu-Washizu and Related Formulations, and Computational Behavior in the Incompressible Limit, Computer Methods in Applied Mechanics and Engineering, Vol.195, 2006, pp. 4161-4178

Lu S, Dong M. An advanced BEM for thermal and stress analyses of components with thermal barrier coating, Electronic Journal of Boundary Elements, 1, 2003, pp. 302-315

Maksimyuk1 VA and Chernyshenko1 IS, Mixed functionals in the theory of nonlinearly elastic shells. Volume 40, Number 11 / November, 2004, International Applied Mechanics, Springer New York

Mijuca D. On hexahedral finite element HC8/27 in elasticity. Computational Mechanics 33(6), 2004, pp.466-480

Mijuca D, Berković M. Stress recovery procedure based on the known displacement, Facta Universitatis, Series Mechanics, Automatic control and Robotics, Vol.7, No.2, 1997, pp. 513-523

Mijuca D, Mastilović S. A Novel One-To-One Multiscale Approach to Computational Mechanics of Materials, 1st International Workshop on Nanoscience & Nanotechnology IWON2005, 2005, pp. 180-186,

Mijuca D, Ziberna A and Medjo B, A Novel Primal-Mixed Finite Element Approach for Heat Transfer in Solids, Computational Mechanics, Computational Mechanics, on-line first, 2006

Prathap G, Naganarayana BP. Consistent thermal stress evaluation in finite elements, Computers and Structures 54, 1995, pp. 415-426

Piltner R, Joseph DS. An accurate low order plate bending element with thickness change and enhanced strains. Computational Mechanics 27: 2001, pp. 353-359

Rannacher R, Suttmeier FT. A feed-back approach to error control in finite element methods: application to linear elasticity, Computational Mechanics. 19(5), 1997, pp. 434-446

Roark RJ, Young WC. Formulas for Stress and strain. McGraw-Hill. Fifth Edition, 1975

Robey TH The Primal Mixed Finite Element Method and the LBB Condition, Numerical Methods for Partial Differential Equations. 8, 1992, pp. 357-379

Shepherd MS, Finite element modelling within an integrated geometric modelling environment: Part II Attribute specification, domain differences and indirect element types. Engineering with Computers 1, 1985., pp.73-85,

Schmauder S Computational Mechanics Annu. Rev. Mater. Res. Vol.32, 2002, pp.437–65

Societe Francaise des Mecanic iens, Commission Validation des progiciels de calcul de Structures, groupe de travail Thermique (2D et 3D) et thermoelasticite: TPLV 04/89. Paris, (1989)

Timoshenko S, Goodier JN, Theory of elasticity, McGraw–Hill, New York, 1970

Wilson EL, Ibrahimbegovic A. Use of incompatible displacement modes for the calculation of element stiffnesses or stresses. Finite Element Anal. Design. 7, 1990, pp. 229-241